Enhancing the Identification of Phosphopeptides from Putative Basophilic Kinase Substrates Using Ti (IV) Based IMAC Enrichment*⑤

Houjiang Zhou‡§, Teck Y. Low‡§, Marco L. Hennrich‡§, Henk van der Toorn‡§, Thomas Schwend‡§, Hanfa Zou¶, Shabaz Mohammed‡§, and Albert J. R. Heck‡§‖

Metal and metal oxide chelating-based phosphopeptide enrichment technologies provide powerful tools for the in-depth profiling of phosphoproteomes. One weakness inherent to current enrichment strategies is poor binding of phosphopeptides containing multiple basic residues. The problem is exacerbated when strong cation exchange (SCX) is used for pre-fractionation, as under low pH SCX conditions phosphorylated peptides with multiple basic residues elute with the bulk of the tryptic digest and therefore require more stringent enrichment. Here, we report a systematic evaluation of the characteristics of a novel phosphopeptide enrichment approach based on a combination of low pH SCX and Ti^{4+}-immobilized metal ion affinity chromatography (IMAC) comparing it one-to-one with the well established low pH SCX-TiO_2 enrichment method. We also examined the effect of 1,1,1,3,3,3-hexafluoroisopropanol (HFP), trifluoroacetic acid (TFA), or 2,5-dihydroxybenzoic acid (DHB) in the loading buffer, as it has been hypothesized that high levels of TFA and the perfluorinated solvent HFP improve the enrichment of phosphopeptides containing multiple basic residues. We found that Ti^{4+}-IMAC in combination with TFA in the loading buffer, outperformed all other methods tested, enabling the identification of around 5000 unique phosphopeptides containing multiple basic residues from 400 μg of a HeLa cell lysate digest. In comparison, ~2000 unique phosphopeptides could be identified by Ti^{4+}-IMAC with HFP and close to 3000 by TiO_2. We confirmed, by motif analysis, the basic phosphopeptides enrich the number of putative basophilic kinases substrates. In addition, we performed an experiment using the SCX/Ti^{4+}-IMAC methodology alongside the use of collision-induced dissocia-tion (CID), higher energy collision induced dissociation (HCD) and electron transfer dissociation with supplementary activation (ETD) on considerably more complex sample, consisting of a total of 400 μg of triple dimethyl labeled MCF-7 digest. This analysis led to the identification of over 9,000 unique phosphorylation sites. The use of three peptide activation methods confirmed that ETD is best capable of sequencing multiply charged peptides. Collectively, our data show that the combination of SCX and Ti^{4+}-IMAC is particularly advantageous for phosphopeptides with multiple basic residues. *Molecular & Cellular Proteomics 10: 10.1074/mcp.M110.006452, 1–14, 2011.*

Reversible protein phosphorylation widely regulates cellular functions through protein kinases and phosphatases (1, 2). Determination and a quantitative analysis of phosphorylation sites are a prerequisite for unraveling regulatory processes and signaling networks (3–6). The analytical methods of choice for characterizing protein phosphorylation have shifted from traditional methods such as radioactive labeling and gel electrophoresis to advanced mass spectrometry, a high-throughput technology (7). It has been estimated that ~30% of cellular proteins are phosphorylated during the life cycle of the cell (8). There has been a continuing intense focus on developing enrichment and phosphopeptide sequencing strategies to facilitate the large-scale profiling of phosphorylation events. Currently, one of the most commonly adopted strategies is the use of two sequential steps of chromatographic based separations; an initial fractionation step for reducing sample complexity and, subsequently, a more specific enrichment of phosphopeptides.

Typically, low-pH strong cation exchange (SCX)[1] chromatography is used as the first step where peptides are fraction-

[1] The abbreviations used are: SCX, strong cation exchange chromatography; Ti^{4+}-IMAC, immobilized titanium (IV) ion affinity chromatography; HFP, 1,1,1,3,3,3-hexafluoroisopropanol; DHB, 2,5-dihydroxybenzoic acid; FDR, false discovery rate; ETD, electron transfer dissociation with supplementary activation; HCD, higher energy collision induced dissociation; CID, collision induced dissociation; PSM, peptide to spectrum match; MS/MS, tandem mass spectrometry.

ated based on their solution net charge (9, 10) and the orientation of peptides to the negatively charged chromatographic material (11, 12). Unlike glutamic and aspartic acid, phosphorylated amino acids are able to retain a negative charge under acidic (pH 2.7) conditions. This property can be exploited in SCX (10) for enrichment of phosphopeptides, which tend to elute earlier and are thus separated from the majority of nonphosphopeptides. Following SCX fractionation, several affinity-based methods have been introduced for improving the level of enrichment including; immobilized metal ion (Fe^{3+}) affinity chromatography (IMAC) (13, 14), and various metal oxides among which TiO_2 is the most common (15, 16). Additional enrichment strategies have also been developed applying different metal oxides such as ZrO_2 and Nb_2O_5 (17, 18) or IMAC using alternative metal ions such as Ga^{3+}, Zr^{4+}, and Ti^{4+} (19–21). Notably, the IMAC technology using Zr^{4+}/Ti^{4+}-metal ions use a phosphate group (as opposed to nitrilotriacetic acid or iminodiacetic acid) as the coordinating ligand that has shown potential to posses superior specificity than traditional metal oxides and Fe^{3+}-IMAC (20, 21) based enrichment strategies. Recently, alternatives to SCX as a first step have also been demonstrated including the use of hydrophilic interaction chromatography (HILIC) (22, 23), electrostatic repulsion liquid chromatography (ERLIC) (24) and strong anion exchange (SAX) (25–27). Although a great number of phosphorylation sites have been identified, it has also been pointed out that each phosphopeptide enrichment technology has inherent biases toward different physiochemical properties of phosphopeptides. For instance, Fe^{3+}-IMAC has been shown to have a more efficient handling of multiply phosphorylated peptides compared with TiO_2. This can be rationalized by the weaker binding to phosphopeptides by IMAC than TiO_2 (28). The specificity and ability to enrich for each method can vary from nearly 100% to a few percent, depending on sample complexity and peptide composition. One weakness common to most chelation strategies is their poor binding to phosphopeptides that contain multiple basic residues (29–32). We argue that this may lead to an underrepresentation of basophilic kinase substrates in current phosphoproteome studies, as these are characterized by high R/K contents in the neighborhood of the phosphorylated residues. The weak representation of phosphopeptides containing multiple basic residues may be caused by an ionic interaction between the basic and phosphorylated residues that hinders the latter's ability to coordinate with the affinity purification by IMAC or metal oxides. Barnouin *et al.* demonstrated that issues relating to intramolecular interactions can be alleviated by switching from a water system to a perfluorinated solvent system (31). However, only simple mixtures were used and specificity was not evaluated using a more complex sample. Another possible way of disrupting the ionic interaction is by increasing the strength of the ion pairing reagent. It has been suggested that elevated levels of TFA will preferably interact with basic residues (33).

Under-representation of phosphopeptides containing multiple basic residues in an SCX-chelation strategy can also be explained by additional factors. Phosphorylated peptides containing multiple basic residues co-elute with the bulk of the digested sample and thus their enrichment is hampered because of the higher complexity and dynamic range issue present in these SCX fractions. These fractions also contain highly acidic peptides, which have been demonstrated in the past to bind to chelation material and reduce specificity. Conversion of carboxylate groups to methyl ester derivates has been demonstrated to improve the selectivity of Fe^{3+}-IMAC (34), although the required chemistry can be problematic.

Sequencing of phosphorylated peptides by tandem mass spectrometry is another key issue that may hamper comprehensive analysis (35, 36). Phosphopeptides are traditionally fragmented by collision induced dissociation (CID). However, phospho-serine and phospho-threonine containing peptides often undergo significant neutral loss of phosphate during CID, giving insufficient backbone fragmentation for phosphopeptide identification (35). Methods such as neutral loss-triggered MS^3 (10) and multistage activation (37) have been employed to impose additional activation events on pre-selected neutral loss peaks. However, there is still discussion whether it is really advantageous to use neutral loss-driven MS^3 and multistage activation scans in phosphoproteomics. Recently, electron capture dissociation (ECD) and electron transfer dissociation (ETD) have shown to be highly complementary to CID because they do not cleave the labile phosphate group, thereby improving the identification of phosphopeptides and localization of phosphorylation sites (38–45).

In this study, we present a systematic evaluation of enrichment of phosphopeptides containing multiple basic residues using SCX-Ti^{4+}-IMAC (21), placing it directly in the context of the SCX-TiO_2 enrichment method which we have helped establish (4, 16, 46). We argue, and show by motif analysis of the phosphopeptide datasets, that our approach is in particular beneficial when there is an interest in the analysis of putative basophilic kinases substrates.

EXPERIMENTAL PROCEDURES

Sample Preparation—HeLa and MCF–7 cells were grown on plates until confluence was reached. After harvesting the cells by scraping, lysis was carried out by resuspending them in lysis buffer containing 50 mM ammonium bicarbonate pH 8.0, 8 M urea. Complete EDTA-free protease inhibitors mixture (Roche) and phosSTOP phosphatase inhibitor mixture (Roche). The cell suspension was subjected to ultrasonication for 1 min at 60 W using 30 cycles with 50% duty. Subsequently, cell debris was removed by centrifugation at $1000 \times g$ for 10 min at 4 °C. Six milligrams of total protein from HeLa cell and 1.2 milligrams of MCF–7 cells were re-suspended in a buffer containing 8 M urea, 50 mM ammonium bicarbonate pH 8.0, reduced with 10 mM dithiothreitol for 30 mins at 56 °C and alkylated by addition of to 20 mM iodoacetamide. After 30 min incubation in the dark at room temperature, the first digestion was performed by addition of Lys-C at an enzyme/protein ratio of 1/50 and incubation for 4 h at 37 °C.

Subsequently, the digest was diluted to a final urea concentration of 2 M, and a second digestion with trypsin at an enzyme/protein ratio of 1/50 was performed at 37 °C overnight. Finally, the digestion was quenched with 0.1% formic acid. The resulting digest of HeLa cells was desalted using 200cc Sep-Pak C18 cartridges (Waters Corporation), dried *in vacuo* and stored at −20 °C. The tryptic digest of the MCF-7 cell lysate was split into three aliquots and then desalted using a 50cc Sep-Pack C18 column, and then washing with 0.1% formic acid. On-column stable isotope dimethyl labeling was sequentially performed, as described before (47). The resulting solution was then dried *in vacuo* and stored at −20 °C. The light, intermediate and heavy dimethyl labeled samples were mixed in a 1:1:1 ratio.

Strong Cation Exchange Chromatography for Peptide Fractionation—The peptides or dimethyl labeled peptides were reconstituted in 10% formic acid and then loaded onto C18 cartridge (Aqua, Phenomenex) using an Agilent 1100 HPLC system. The flow rate applied was 100 μL/min using 0.05% formic acid (pH 2.7) as solvent. Peptides were eluted from the C18 cartridge with 80% acetonitrile (ACN)/0.05% formic acid (pH 2.7); onto a Polysulfoethyl A column (200 × 2.1 mm) (PolyLC) for 10 min at the same flow rate. Separation of peptides was performed at using a nonlinear 65 min gradient: from 0 to 10 min, 100% solvent A (5 mM KH_2PO_4, 0.05% formic acid, 30% acetonitrile, pH 2.7); from 10 min to 15 min, to 26% solvent B (5 mM KH_2PO_4, 0.05% formic acid, 30% acetonitrile, 350 mM KCl, pH 2.7); from 15 min to 40 min, to 35% solvent B; and from 40 to 45 min, to 60% solvent B. At 49 min, the concentration of solvent B was 100%. The column was subsequently washed for 6 min with 100% solvent B and finally equilibrated with 100% solvent A for 9 min. The flow rate applied during the SCX gradient was 300 μL/min. Fractions were collected every minute for 40 min. Each fraction was lyophilized and then desalted by resuspension in 2% acetic acid using 50cc Sep-Pak C18 cartridges (Water Corporation). The eluted peptides from each fraction were split into five aliquots, lyophilized and stored at −20 °C. The dimethyled labled peptides from each fraction were also desalted, dried *in vacuo* and stored at −20 °C.

Phosphopeptide Enrichment—Ti^{4+}-IMAC material was prepared and used essentially as previously described by us (21, 48). Titansphere (GL Science) microcolumns were prepared as previously described (16, 49). Affinity material (TiO_2 and Ti^{4+}-IMAC resin) was loaded onto Gel-loader tip microcolumns using a C8 plug and ~1–2 cm length of material. The enrichment procedures for "positive" SCX fractions of tryptic digest of HeLa cell were as follows: first, Pre-equilibrated by 2 × 30 μL of TiO_2 loading buffer (Approach TiO_2^a: 80% ACN, 0.1% TFA with 50 mg/ml DHB or approach TiO_2^b: 80% ACN, 6% TFA with 50 mg/ml DHB) for TiO_2 columns, 2 × 30 μL of Ti^{4+}-IMAC loading buffer (Approach Ti^{4+}-IMAC^a: 80% ACN, 6% TFA) to Ti^{4+}-IMAC column, 2 × 30 μL of Ti^{4+}-IMAC loading buffer (Approach Ti^{4+}-IMAC ^{b}: 60% HFP, 0.1% TFA) for Ti^{4+}-IMAC column,. Next, four aliquots of each SCX fraction were, re-suspended in 60 μL of loading buffer each and loaded onto the equilibrated gel-loader tip microcolumns. Columns were sequentially washed with 60 μL of loading buffer, followed by washing with 60 μL of 50% ACN/0.1% TFA for TiO_2 columns, 60 μL of 50% ACN/0.5% TFA containing 200 mM NaCl for Ti^{4+}-IMAC^a column and additional washing by 60 μL of 50% ACN/0.1% TFA for Ti^{4+}-IMAC^a and Ti^{4+}-IMAC^b columns, respectively. The bound peptides were eluted by 20 μL of 5% ammonia into 20 μL of 10% formic acid and then stored at −20 °C for LC-MS/MS analysis. The same procedures were performed for phosphopeptide enrichment from neutral phosphopeptide-enriched SCX fractions and whole unfractionated digests of HeLa lysate. For the SCX fractions of the dimethyl labeled of MCF-7 cell lysate enrichment was performed using the Ti^{4+}-IMAC^a strategy.

Mass Spectrometry—The analysis of the peptides was performed on a reversed phase (RP) nano-LC-coupled LTQ Orbitrap XL ETD

(Thermo Fisher Scientific) as described previously with minor modifications (50). An Agilent 1200 series HPLC system was equipped with a 20 mm Aqua C18 (Phenomenex, Torrance, CA) trapping column (packed in-house, 100 μm i.d., 5 μm particle size) and a 400 mm ReproSil-Pur 120 C18-AQ (Dr. Maisch-GmbH) analytical column (packed in-house, 50 μm i.d., 3 μm particle size). Trapping was performed at 5 μl/min solvent C (0.1 M acetic acid in water) for 10 min, and elution was achieved with a gradient of 10–25% (v/v) solvent D (0.1 M acetic acid in 80% ACN) in 90 min with a total analysis time of 120 min. The flow rate was passively split from 0.60 ml/min to 100 nL/min when performing the elution. Nanospray was achieved using a distally coated fused silica emitter (360 μm o.d., 20 μm i.d., 10 μm tip i.d.; constructed in-house) biased to 1.7 kV. The LTQ Orbitrap ETD was operated in the data dependent mode to automatically switch between MS and MS/MS. Survey full scan MS spectra were acquired from *m/z* 350 to *m/z* 1500 in the Orbitrap with a resolution of 60,000 at *m/z* 400 after accumulation to a target value of 500,000 in the linear ion trap. Supplementary activation was enabled for ETD (51). The five most intense peaks at a threshold of above 500 were alternatively fragmented in the linear ion trap using CID/ETD at a target value of 30,000. The ETD reagent target value was set to 100,000 and the reaction time to 50 ms.

The enriched phosphopeptides from dimethyl labeled samples were analyzed on an ETD equipped Orbitrap Velos instrument (Thermo Fisher Scientific, Bremen) connected to an LC system as described above. All instrument methods for the Orbitrap Velos were set up in the data dependent acquisition mode. Each sample was analyzed with either a Top10 HCD or Top10 CID/ETD method. For the low-resolution CID/ETD-MS/MS method, full scan MS spectra (from *m/z* 350–1500) were acquired in the Orbitrap analyzer after accumulation to a target value of 5e5 in the linear ion trap. Resolution in the Orbitrap system was set to 60,000. The ten most intense peptide ions were sequentially isolated to a target value of 5000 and fragmented in the high-pressure linear ion trap by low-energy CID with normalized collision energy of 35%. The ETD reagent target value was set to 2e5 and the reaction time to 100 ms. For the HCD method, survey full scan MS spectra (from *m/z* 350–1500) were acquired in the Orbitrap system with resolution 30,000. The ten most intense peptide ions were sequentially isolated to a target value of 3e4 and fragmented in the HCD collision cell with normalized energy of 35%. The resulting fragments were detected in the Orbitrap with resolution 7500.

Data Analysis—From each raw data file recorded by the mass spectrometer, representing the enriched phosphopeptide from each SCX fraction, peak lists containing CID, ETD and HCD fragmentation data were generated using Proteome Discoverer (Version 1.3, Thermo Fisher Scientific) with a signal-to-noise threshold of 3 and the following settings for the ETD nonfragment filter: precursor peak removal within a 4 Da, charge-reduced precursor removal within a 2 Da, and removal of known neutral losses from charge-reduced precursor within a 2 Da (the maximum neutral loss mass was set to 120 Da). Single-fraction peak lists generated from each method were then merged into one larger peak list for database searching using in-house scripts, in which CID peak lists was further filtered as minimum fragment ions was set to 100, maximum number of fragment ion count was set to 100, maximum number of fragment ions was set to 100. Peak list files from HCD were deisotoped and charge deconvoluted as described (52, 53). Peak lists were searched against a IPI human database (version 3.52, 69,164 sequences; 29,064,824 residues) and its decoy database created by Mascot using Mascot software version 2.3.02 (Matrix Science, UK). The database search was performed with the following parameters: a mass tolerance of ±50 ppm for precursor masses and ±0.6 Da for CID/ETD fragment ions and ±0.05 Da for HCD fragments, allowing two missed cleavages, cysteine carbamidomethylation as fixed modification and methionine

oxidation, phosphorylation of serine, threonine, and tyrosine as variable modifications. When the data was triple dimethyl labeled peptides, additional variable modifications relating to the N terminus and Lysine residues were also added. The enzyme was specified as trypsin and the fragment ion type was specified as electrospray ionization (ESI)-TRAP, ETD-TRAP, and ESI-quadrupole-time-of-flight (Q-TOF) for the corresponding mass spectra. The resulting .dat files were exported and filtered for a <1% false discovery rate (FDR) at the peptide level using in-house developed software "Rockerbox" (Version 1.2.6) (54) utilizing the percolator-based algorithm (55). Note, only PSMs with Mascot score ≥20 were accepted and then exported using "Rockerbox" (54). Site localization confidence was calculated using mascot delta score (43), which has been reported to be a viable method by Savitski and coworkers (56). The frequency of amino acids within identified phosphopeptides was performed using the IceLogo program (57), which builds on probability theory to visualize significant conserved sequence patterns in multiple peptide sequence alignments against background sequence sets and has a more dynamic nature and is correct and completer in the analysis of conserved sequence patterns, was used to analyze the frequency of amino acids. Note: considering the possibility of missed cleaved peptides, the peptide sequences were extended to 21 amino residues window surrounding the center of phosphorylation S/T/Y sites.

All of the data sets can be accessed as scaffold data files (www. proteomesoftware.com) at the publicly available repository Tranche (https://proteomecommons.org/) using the following hash code: p9mbfyL44qFNOl4ejNDmC+/wwGbPvnSQVsj6yueyNfOEla-q84opm09URtLWGtaaqulI+c6pQjMK+5F2zghoogxtOJ/IAAAAAAA-ADKA = = .

RESULTS

Effect of Organic Additives on Phosphopeptides Enrichment by TiO₂ and Ti⁴⁺-IMAC—Our main objective was to develop a phosphoproteomics method specifically improving enrichment of phosphopeptides containing multiple basic residues, enabling the expansion of global phosphoproteome profiles. Applying a low pH (2.7) SCX separation on a lysate allowed the fractionation of peptides based on charge state, resulting from protonation and deprotonation of basic and acidic groups. It is estimated that ∼68% of an *in silico* tryptic digest of the human IPI protein database generates peptides with a net charge of 1+ under pH 2.7 assuming protonation of both the N terminus and the basic residue and deprotonation of the C terminus (9). Such tryptic peptides are often referred to as "2+" in the literature (ourselves guilty) which ignores the deprotonation of the C terminus that has an important impact on the separation (12). Phosphopeptides containing only one basic residue will have a net charge of zero (protonation of the N terminus and the basic residue combined with deprotonation of the C terminus and phosphorylated residue) and will elute earlier in an SCX based separation. For the sake of simplicity we will refer to these as "neutral phosphopeptides". Phosphopeptides containing more than one basic residue will have a net charge corresponding to the number of basic residues minus one and for simplicity these positively charged phosphopeptides will be referred to as "positive phosphopeptides". Note that the "positive phosphopeptides" will co-elute with regular tryptic peptides that also possess a net positive charge. The reference sample we tested was a HeLa cell lysate digest (6 mg), which was initially fractionated by SCX. Each of these SCX fractions was divided into five aliquots for further experiments. Initially, single aliquots of the fractions containing positively charged peptides were pooled together and used as an initial test bed for optimizing enrichment protocols. It is noteworthy that all SCX fractions were desalted before enrichment to eliminate any deleterious effects caused by the phosphate present in the SCX solvents. Previously, Cramer and coworkers suggested that fluorinated solvents such as HFP can significantly improve "positive phosphopeptides" enrichment by reducing the level of intramolecular ionic interaction (31). Using this work as a reference, where it was suggested 40% HFP would be beneficial, we tested a range of organic solvents differing in their HFP (40, 60, and 80%) and TFA content (0 and 0.1%). Both TiO₂ and Ti⁴⁺-IMAC enrichment protocols were tested. It was observed that the optimal loading buffer is 60% HFP with 0.1% TFA for Ti⁴⁺-IMAC whereas the results for TiO₂ were much poorer than the classical solvent system (See [supplemental Table S1](#)). These initial findings were then used for a much larger and refined experiment.

Comparative Evaluation of TiO₂ and Ti⁴⁺-IMAC Enrichment of Phosphopeptides—Aliquots of each of the SCX fractions corresponding to positively charged peptides were subjected to enrichment by TiO₂ and Ti-IMAC using several solvent systems that will help evaluate the use of TFA, DHB and HFP. In order to be consistent we created two enrichment methods for TiO₂, one containing DHB (the classic strategy and termed TiO2ᵃ) and one containing 6% TFA (to mimic the classical conditions used for Ti-IMAC, termed TiO2ᵇ). Two Ti-IMAC methods were also used; Ti⁴⁺-IMAC with 6% TFA (termed Ti⁴⁺-IMACᵃ) and Ti⁴⁺-IMAC with 60% HFP and 0.1% TFA (termed Ti⁴⁺-IMACᵇ). The SCX fractions were subjected to enrichment by each method and then one-third of the enriched eluent (corresponding to a total lysate level of 400 μg) was analyzed by LC-MS/MS where each precursor was subjected to both CID and ETD fragmentation events. An overview of the experimental strategy is shown in Fig. 1. The four methods TiO₂ᵃ, TiO₂ᵇ, Ti⁴⁺-IMACᵃ, and Ti⁴⁺-IMACᵇ yielded 588, 2990, 4749, and 1846 unique phosphopeptide identifications originating from 430, 1534, 1939, and 929 phosphoproteins, respectively (Table I and [supplemental Tables S2, S3, S4 and S5](#)). In addition, the specificity of phosphopeptide enrichment was in the order of Ti⁴⁺-IMACᵃ > TiO₂ᵇ > Ti⁴⁺-IMACᵇ > TiO₂ᵃ (Table I). Considering that the TiO₂ᵇ method identified more phosphopeptides than the TiO₂ᵃ method, only the phosphopeptides identified using the TiO₂ᵇ method were further analyzed and compared with the Ti⁴⁺-IMAC approaches. Comparing overlap of the 3 methods clearly indicated that 6% TFA in conjunction with Ti⁴⁺-IMAC, Ti⁴⁺-IMACᵃ, was superior and most comprehensive (Fig. 2A). 1321 unique phosphopeptides representing 21.7% of all phosphopeptides were solely identified by the TiO₂ᵇ and Ti⁴⁺-IMACᵃ approaches. It should be pointed out that the use of
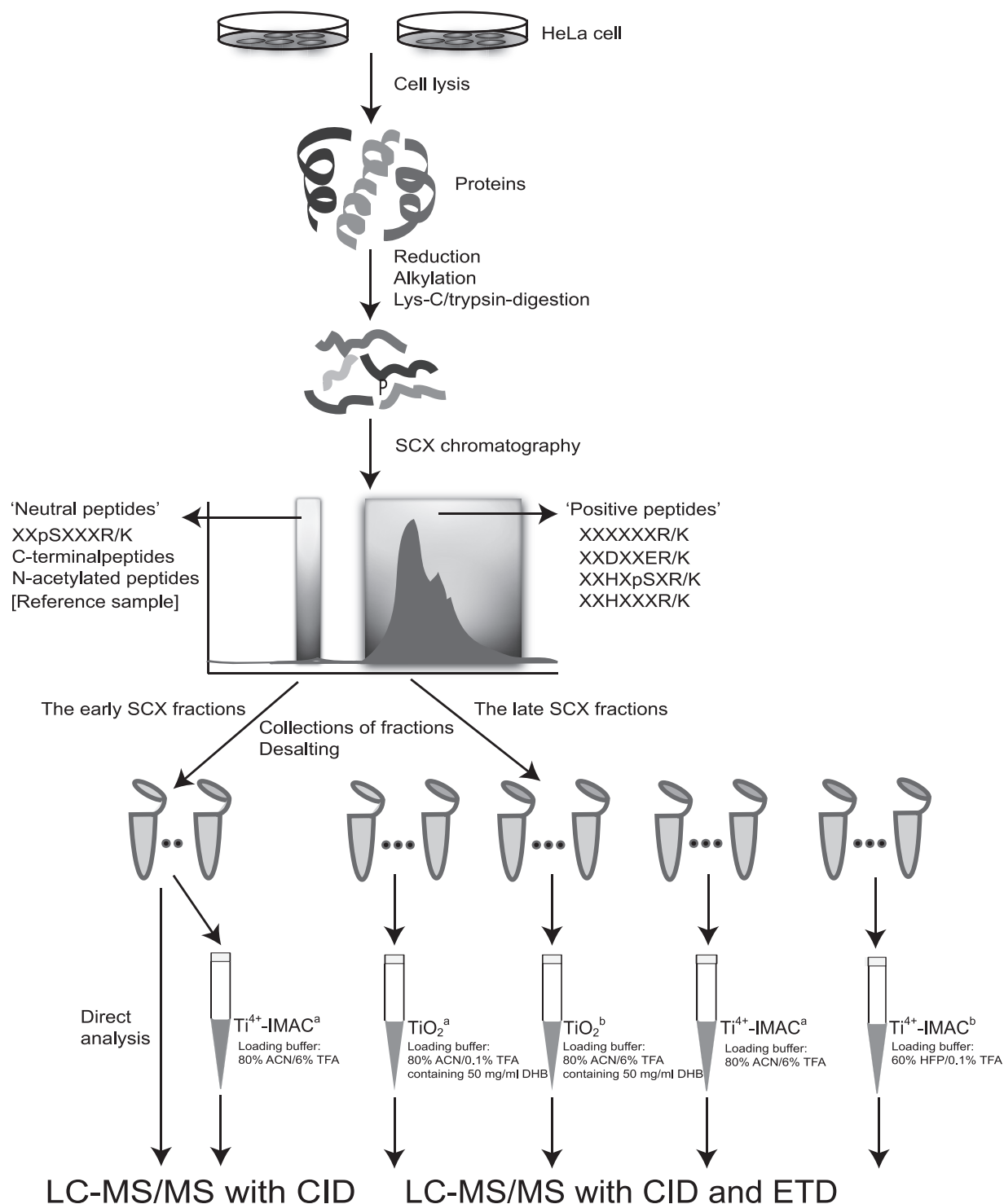
FIG. 1. **Experimental workflow used for the selective enrichment and identification of phosphopeptides.** A HeLa lysate tryptic digest was initially fractionated by SCX. After desalting and aliquoting the SCX fractions, the late SCX fractions (containing the bulk of the tryptic peptides, and the phosphopeptides with multiple basic residues), were subjected to TiO_2 (Approach TiO_2[a]: 80% ACN/0.1% TFA containing 50 mg/ml DHB used as loading buffer; Approach TiO_2[b]: 80% ACN/6% TFA containing 50 mg/ml DHB used as loading buffer), Ti^{4+}-IMAC (Approach Ti^{4+}-IMAC[a]: 80% ACN/6% TFA used as loading buffer; Approach Ti^{4+}-IMAC[b]: 60% HFP/0.1% TFA used as loading buffer) enrichment. The eluant was, subsequently, analyzed by LC-MS/MS utilizing both CID and ETD. The early SCX fractions were also analyzed, either directly but also after Ti^{4+}-IMAC[a] enrichment, albeit by using CID only.

Overview of phosphorylated peptides identified with each of the used methods, for the analysis of the late (positive peptides) and early (neutral peptides) SCX fractions. The late SCX fractions contain the bulk of "normal" tryptic peptides

Sample used	Approach	Phosphopeptides			Summary		
		CID	ETD	Unique phosphopeptides	Unique phosphorylation sites	Phosphoproteins	Specificity
The late SCX Fraction	TiO_2^a	435	366	588	633	430	3%
	TiO_2^b	2177	1287	2990	3075	1534	46%
	Ti^{4+}-$IMAC^a$	2814	3890	4749	4814	1939	63%
	Ti^{4+}-$IMAC^b$	832	1558	1846	1980	929	38%
The early SCX Fraction	Ti^{4+}-$IMAC^a$	3246		3246	3354	1743	98%
	Direct analysis	1883		1883	2054	1145	88%

* The threshold for accepted phosphopeptide identifications was taken at mascot score at least 20 corresponding to an FDR of <1%.

FIG. 2. **Multipronged phosphoproteomics analysis of a HeLa lysate using the workflow described in Fig. 1.** Venn diagrams displaying the overlap in detected (unique) phosphopeptides for (A) phosphopeptides detected in the late SCX fractions corresponding to peptides with a positive charge using the enrichment methods TiO_2^a, Ti^{4+}-$IMAC^a$ and Ti^{4+}-$IMAC^b$, respectively (B) phosphopeptides detected in the early SCX fractions containing peptides with a net neutral charge either through direct analysis or after the additional enrichment using Ti^{4+}-$IMAC^a$.
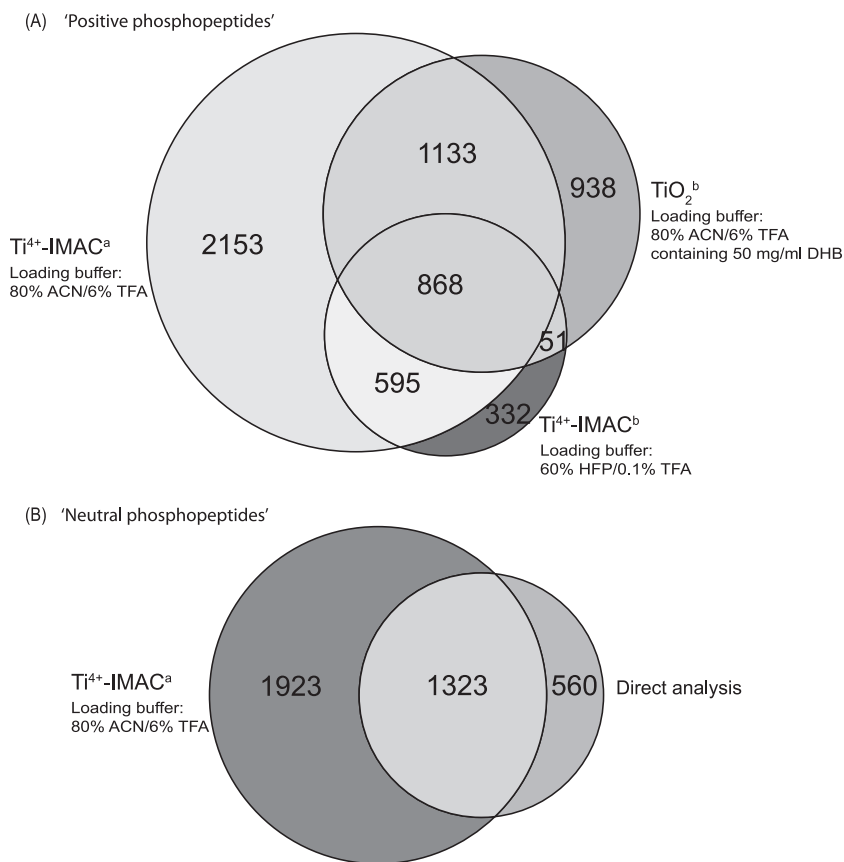
SCX and TiO_2/Fe^{3+}-IMAC for the enrichment of "neutral phosphopeptides" is superb, leading to the generation of nearly pure pools of phosphopeptides (13–15, 58). In contrast, TiO_2 performs here relatively poorly for "positive phosphopeptides," in line with what has been previously pointed out (29, 32). In order to generate a reference to allow a more in-depth evaluation of the positive phosphopeptide pools and to confirm that Ti^{4+}-$IMAC^a$ can also generate similar results to TiO_2, a portion of the SCX fractions corresponding to where "neutral phosphopeptides" are found were also subjected to enrichment. Four of these SCX fractions were further purified by TI^{4+}-$IMAC^a$ approach, generating a data set of 3246 unique phosphopeptides from 1743 phosphoproteins (supplemental Table S6).

We further compared the number of unique phosphopeptides recovered from the early SCX fractions and those originating from later SCX fractions after enrichment with TI^{4+}-$IMAC^a$ approach. We found, as anticipated, little overlap in phosphopeptide identifications in between these early and late SCX fractions because of the separation power of SCX. In addition, direct analysis of these four fractions without enrichment resulted in the identification of 1883 unique phosphopeptides originating from 1145 phosphoproteins (supplemental Table S7). When comparing the data set obtained by direct analysis after SCX enrichment and that obtained after subsequent enrichment by Ti^{4+}-$IMAC^a$, it became apparent that the additional enrichment is also beneficial for the early SCX fractions, nearly doubling the
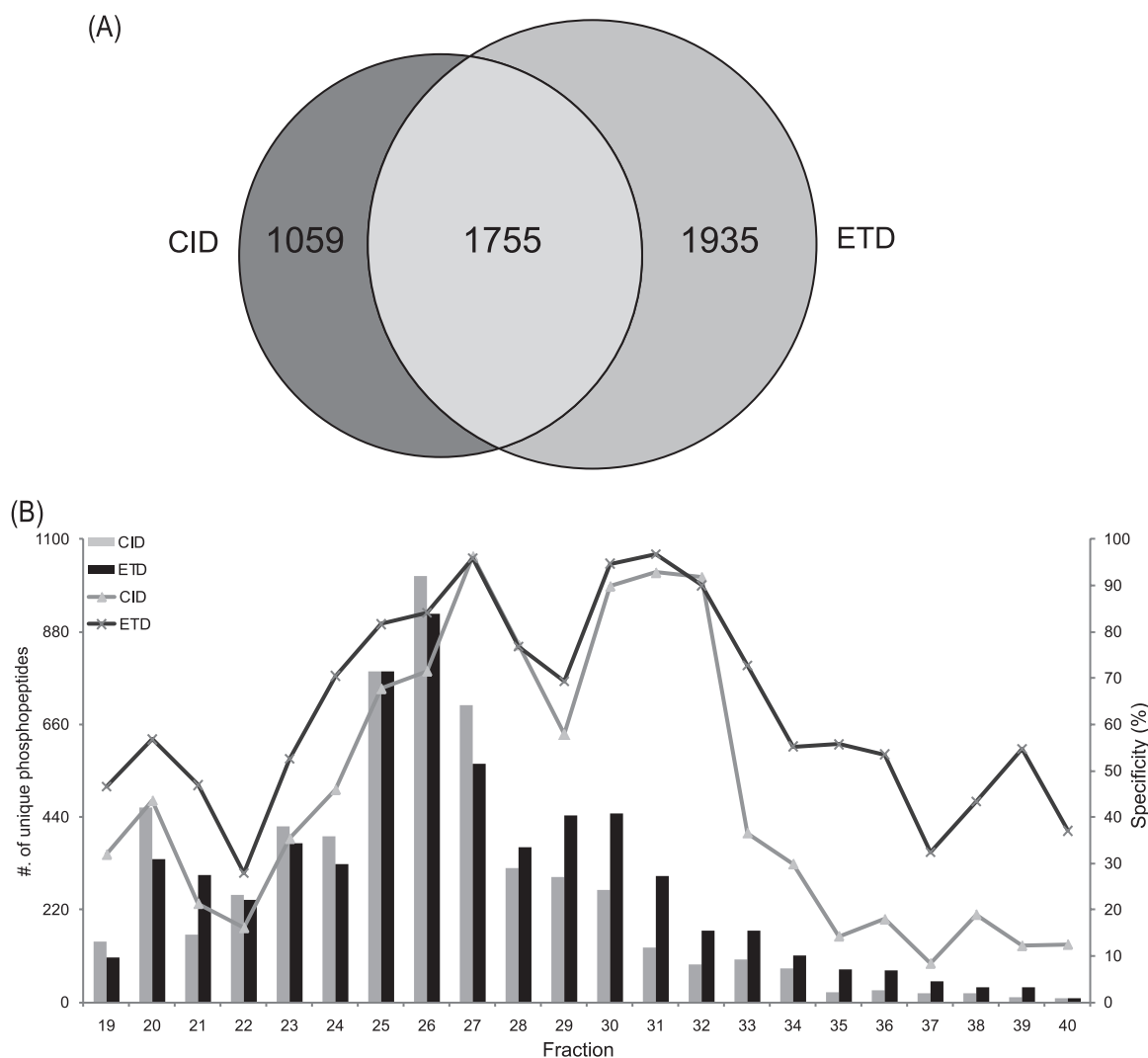
(A)

(B)

Fig. 3. **Comparison of the identified "positive phosphopeptides" using CID and ETD as observed in the HeLa lysate Ti^{4+}-IMAC^a data set.** *A*, Venn diagram indicating the overlap between the phosphorylated peptides identified by CID and ETD (*B*) Bar diagram representing the unique phosphopeptides detected by CID and ETD for each SCX fraction analyzed, coupled to the left *y* axis. Gray and black bars indicate the number of phosphopeptides identified by CID and ETD, respectively. In addition, the line diagrams represent the specificity of identified phosphopeptides per SCX fraction, by CID (*gray*) and ETD (*black*), coupled to the right *y* axis.

amount of detected phosphopeptides (Fig. 2*B*). The level of results for the direct analysis are largely made possible by the separation of the N-acetylated peptides away from the phosphorylated peptides by SCX (12). Interestingly, the enrichment factor without Ti^{4+}-IMAC was close to 90% and with enrichment was close to 100%, according to the results generated by Mascot.

ETD Fragmentation Improves Phosphopeptide Identification, in Particular, of Positive Phosphopeptides—All enriched fractions were analyzed by LC-MS/MS with alternating CID and ETD fragmentation. For the Ti^{4+}-IMAC^a experiment, CID and ETD contributed to the identification of 2814 and 3690 unique phosphopeptides, respectively (Fig. 3*A*). A total of 1755 unique phosphopeptides were commonly identified by both fragmentation techniques, corresponding to an overlap

of only 37%. ETD generated more (41%) identifications than CID. When combined, the two dissociation approaches resulted in the identification of 4749 unique phosphopeptides, corresponding to 4814 unique phosphorylation sites. We further investigated the performance of CID and ETD by breaking down results obtained per individual SCX fraction (Fig. 3*B*). Our analysis indicates that, for individual fractions, CID and ETD identified differing numbers of phosphopeptides as well as generating different 'apparent' phosphopeptide specificities, ranging from 10% percent to 100%. Not only did ETD contributed to more identifications, it also resulted in a higher specificity being calculated for positive phosphopeptide enrichment by the Ti^{4+}-IMAC^a method. An observation that can be rationalized by the known higher efficiency of ETD in fragmenting phosphopeptides with a higher charge where the

higher charge is a product of the presence of multiple basic residues (38, 39, 45).

Comparison of Amino Acid Frequency of the Identified Positive Phosphopeptides and Neutral Phosphopeptides—To investigate the amino acid composition of phosphopeptides obtained for each method, we plotted the frequency of amino acids surrounding the phosphorylation site against a pooled data set consisting of all five data sets as background (Table. 1) using the freeware program Ice Logo (57). This background pooled data set contained a total of 8924 unique phosphorylated peptides.

Tryptic phosphopeptides have been reported to have an average length of 16 amino acids and also tend to harbor more missed cleavages. It has been reported that on average 1.1 missed cleavages per phosphopeptide are observed whereas for regular peptides the average is 0.3 (38). To accommodate for these trends, sequences of 21 amino acids surrounding all identified phosphorylated S/T/Y residues were analyzed. In Fig. 4 each panel represents a data set from a single experimental approach, against a background data set containing all datasets. Ice Logo plots represent enrichment of amino acids as positive values, whereas underrepresented amino acids occur as negative values, keeping in mind that for these data sets there will be two basic amino acids present in each sequence. Each data set generated a unique frequency for amino acids surrounding the phosphorylation site. We found overrepresentation of the basic amino acids R, K and H in proximity to phosphorylated residues for the TiO_2^b strategy (Fig. 4*A*). The frequency of arginine occurrence at positions P-2, P-3, and P-4 was increased more than 5% ($p < 0.01$) and also the basic amino acids K and H were overrepresented. A possible reason for these observations is that the proximity of phosphorylated residues to K/R can hamper the efficiency of trypsin digestion as suggested by others (38, 59, 60). For the Ti^{4+}-$IMAC^b$ strategy (Fig. 4*B*), surprisingly, acidic amino acids of aspartic acid and glutamic acid are more frequently overrepresented ($p < 0.05$) along the peptide backbone. The basic amino acids are marginally overrepresented. Interestingly, proline which is a common member for several kinase substrate motifs, is markedly underrepresented in the position of $p + 1$. If a proline is adjacent to a phosphosite which is not close to a basic residue then trypsin is unhindered whereas if a proline is adjacent to a lysine or arginine then trypsin maybe hindered. Our data suggests that prolines are often close to phosphosites and sufficiently far away from basic residues leading to the generation of a neutral phosphopeptide. The logo generated by Ti^{4+}-$IMAC^a$ approach has a similar pattern to the TiO_2^b strategy, in which the basic amino acids of H, R and K and acidic amino acids of D and E are overrepresented (Fig. 4*C*). On closer inspection, the occurrence of basic amino acids is slightly higher than that for acidic amino acids (5% to 3%). It was also observed that Rs are more frequently enriched at P-2, P-3, and P-4. However, D and E have higher occurrence in the proximity on the right side ($p + 1…p + 5$) of

phosphorylation sites. Strikingly, there is also a clear enrichment of phosphopeptides containing histidines, a pool of peptides that are not a by-product of an incomplete digestion and thus potentially represent a new set of phosphopeptides. However, the neutral phosphopeptide pool generated with Ti^{4+}-$IMAC^b$ enrichment produced a different pattern with the residue proline overrepresented (Fig. 4*D*). Proline direction is common in phosphorylation motifs and, as expected, it is enriched at $p + 1$. Finally, both basic residues and acidic residues showed depletion.

Specific Enrichment of Phosphopeptides Originating From Putative Basophilic Kinase Substrates—Protein kinase target substrates typically depends on the primary amino acid sequence proximal to the site that will be modified (3). The identification of kinase specific substrates can be evaluated using such sequence motifs. Here we performed such a motif-dependent categorization of the detected phosphopeptides for both, albeit separately, the "positive" and "neutral" phosphopeptides enriched by Ti^{4+}-$IMAC^a$ using the motif classification tool implemented in Maxquant (61). In the positive phosphopeptide and neutral phosphopeptide data sets, the algorithm available within Maxquant defined a preferred kinase to 1832 and 985 phosphopeptides, respectively. In Fig. 5*A*, a summary is displayed of the relative contribution of each kinase to the total data set, ignoring kinases that contributed less than 1% to the full data set. Significantly, substrates of different kinases are overrepresented when comparing these two data sets. Most obviously, there is an $\sim$2-fold higher enrichment of peptides originating from putative basophilic kinase substrates such as PKA, PKA/AKT and AURORA in the positive phosphopeptide data set (Fig. 5*B* and 5*C*). Basophilic kinase substrates only contributed to a mere 11% in the neutral phosphopeptide data set (Fig. 5*B* and 5*C*).

An Evaluation of the SCX/Ti^{4+}-$IMAC^a$ Strategy Using a Triple Dimethyl Labeled Lysate—To further evaluate the use of SCX/Ti^{4+}-$IMAC^a$ approach for quantitative phosphoproteomics where complexity is increased because of the introduction of isotope labels, we performed a phosphorylation analysis on a total of 400 μg of dimethyl labeled tryptic digests of MCF-7 cell lysate. A total of 35 fractions were generated using SCX, each of which was subjected to phosphopeptide enrichment via the Ti^{4+}-$IMAC^a$ approach. After enrichment, the eluate of each fraction was analyzed on an LTQ-Orbitrap Velos mass spectrometer by using either HCD or alternating CID and ETD. The data was filtered to <1% FDR using "Rockerbox" (54), which contains percolator (55). The data was further filtered to solely possess PSMs with a minimum mascot score of 20. Next, if a phosphosite was identified more than once, we performed two stages of filtering. Initially, the PSMs corresponding to the earliest fraction were kept. Subsequently, the PSM corresponding to the highest score was kept regardless of the activation technique. supplemental Table S8 contains the final filtered results, summarized in Fig. 6. A total of 9117 unique phosphorylation sites
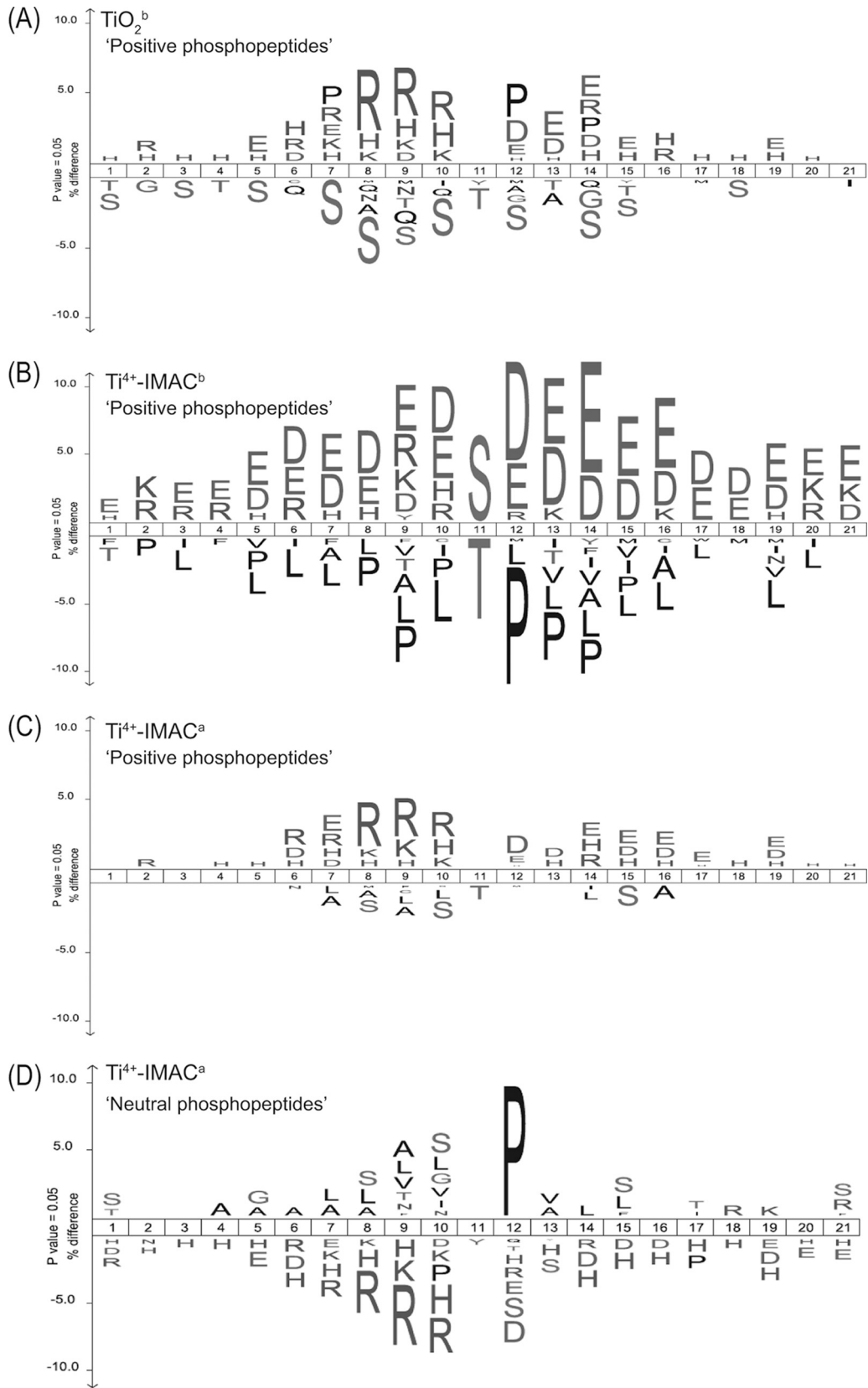
FIG. 5. **Putative kinase specific substrates present in the phosphopeptide data sets generated by Ti^{4+}-IMAC^a enrichment.** *A*, The bar chart shows the classification and distribution of substrates of different kinases found in the "positive phosphopeptide" pool (displayed with *black* bar) whereas the *gray* bars indicate those found in the "neutral" phosphopeptide pool. *B* and *C*, The pie chart shows the distributions of basophilic (*black*) and other kinases (*gray*) in the "positive" and "neutral" phosphopeptide data set, respectively.
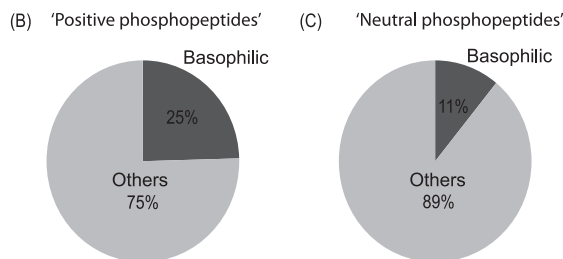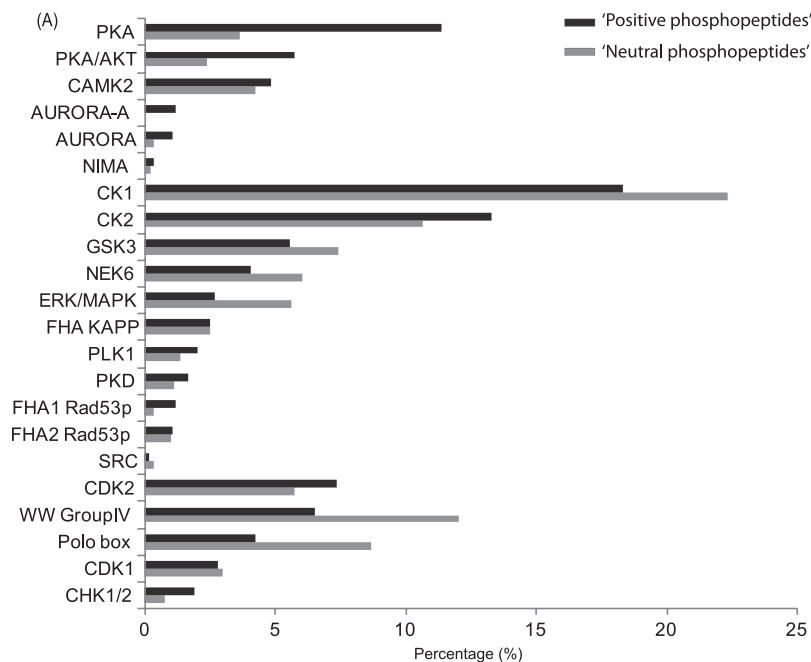
on 9678 unique phosphopeptides was identified (supplemental Table S8). Strikingly, 5300 unique phosphorylation sites (58% of the total) were identified from the later SCX fractions (28–40) corresponding to the positive phosphopeptides. The filtering applied means any site observed in an earlier fraction would be the only site reported. Thus, if we observed the same site in two distinct peptides the peptide observed in the later fraction would be removed regardless of its score. A side effect of this filtering strategy is that it discriminates against phosphopeptides containing miss cleavages. The contribution to the unique phosphopeptide identifications per fraction broken down by activation technique are shown in Fig. 6*B*. As we have recently reported for regular peptides (53), HCD and CID were most effective for the earlier SCX fraction which contain peptides of lower net charge state, and the peptides carrying on 2+ charge. For the late SCX fractions, particularly fractions 34–40, ETD outperformed HCD and CID, contributing 76% of the phosphopeptide identifications.

DISCUSSION

In recent years the combination of SCX and metal chelating enrichment strategies have enabled the large scale analysis of phosphoproteomes, identifying several thousands of phosphorylation sites (3–5, 38, 39). Notwithstanding this success, several issues hampering comprehensive analysis have remained relatively unaddressed. First of all, different affinity-based enrichment technologies have inherent biases often dependent on certain physicochemical properties of the diverse pool of phosphorylated peptides. Another issue is the relatively poor enrichment of phosphopeptides containing multiple basic residues. Poor binding of positive phosphopeptides was suggested to be caused by the intra-peptide interaction between the basic and phosphorylated residues (31), which hinders the ability to coordinate with the affinity material. For instance, Klemm and coworkers found drastically reduced recovery for synthetic phosphopeptides with multiple

FIG. 4. **Frequency distribution of specifically enriched (+) or depleted (-) amino acids, surrounding the site of phosphorylation (position 11), in the HeLa lysate phosphopeptide datasets.** To display theses distributions Ice Logos were generated for each data set using all our phosphoproteomics data as background. The data sets originating from the late SCX fractions are represented in (*A*) TiO$_2$^{a}, (*B*) Ti^{4+}-IMAC^b, and (*C*) Ti^{4+}-IMAC^a. For comparison, in (*D*) the IceLogo for the Ti^{4+}-IMAC^a data set obtained from the early SCX fractions is represented.
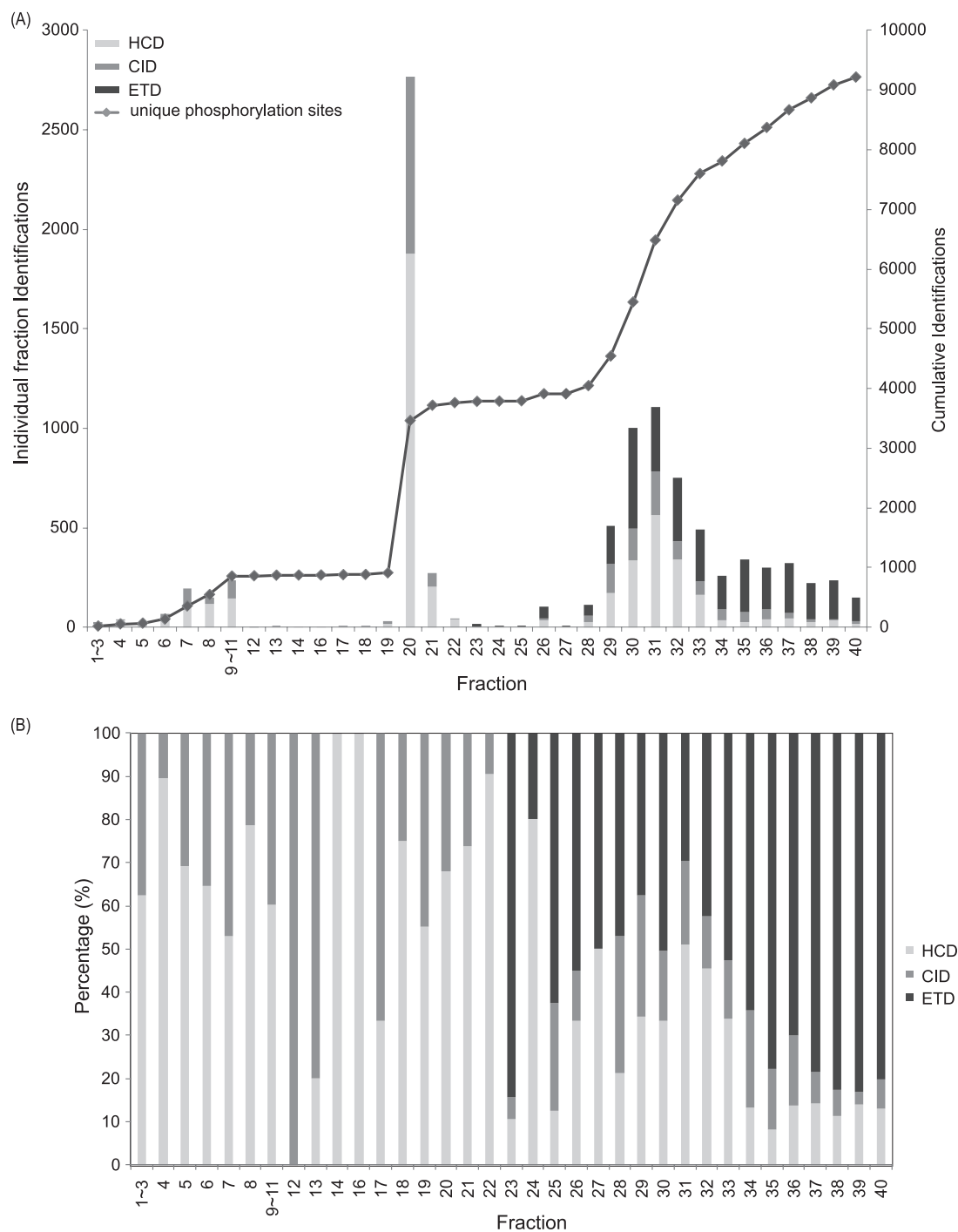
Fig. 6. **Evaluation of the SCX/Ti^{4+}-IMAC approach applied to a triple dimethyl labeled MCF-7 cell lysate digest.** *A,* Bar diagram representing the individual phosphopeptides identified per fraction and the fragmentation method by which it was identified. The accumulation of unique phosphorylation sites resolved by fraction are plotted as a dotted line using the right hand *y* axis. *B,* The contribution of phosphopeptides identified by HCD, CID, or ETD in each fraction. HCD identifications are shown in light *gray*. CID identifications are shown in gray. ETD identifications are shown in *black*.

basic amino acids using TiO$_2$ enrichment (29). Comparative evaluation of the recovery of a basic tyrosine-phosphorylated angiotensin II peptide by Iliuk and coworkers yielded only 25% recovery from a Fe^{3+}-IMAC resin and 50% after TiO$_2$ enrichment (32). The problem in enriching these phosphopep-

tides containing multiple basic residues is further exacerbated because these phosphopeptides require typically the most stringent enrichment as they, in SCX, co-elute with the bulk of the regular tryptic peptide population. Importantly, many basophilic kinases such as those in the AGC kinase family (*e.g.*

PKA, PKG, Aurora) are to a great extent directed by flanking basic amino acids. The current lack of a solution to enrich these basic phosphopeptides can restrict the profiling of phosphorylation sites in particular related to these cellular pathways. Earlier, Barnouin *et al.* has proposed the use of the perflourinated solvent HFP to improve the enrichment of basic phosphopeptides by Fe^{3+}-IMAC (31). However, a systematic evaluation of HFP on enrichment for phosphopeptides containing multiple basic residues at the proteome level was not performed. A recently introduced enrichment technology known as Ti^{4+}-IMAC was shown to have a higher inherent specificity for phosphopeptide enrichment using solely a high level of TFA (21) and without the need of additives, in contrast to the case of TiO_2 (21). In this study, we sought to evaluate Ti^{4+}-IMAC and TiO_2 in conjunction with the perfluorinated solvent (HFP) and/or TFA for improving the enrichment for positive phosphopeptides eluting in the late SCX fractions. Our results showed that Ti^{4+}-IMAC[a] (containing 6% TFA) is capable of achieving both the largest number of identification of positive phosphopeptides and the highest specificity (63%) of enrichment for the late SCX fractions compared with Ti^{4+}-IMAC[b] (38%) and TiO_2[b] (46%). Interestingly, TiO_2[b] (containing 6% TFA) outperformed TiO_2[a] (the classical DHB centric approach). To investigate the characteristic of identified phosphopeptides by different approaches and from different phosphopeptide populations, we initially performed a pI analysis for all datasets, however; each data set revealed a similar pI profile (supplemental Fig. S1), reflecting pattern similar to those of others who also applied SCX/TiO_2 for phosphoproteomics (5, 27). The lack of insight generated by the pI plots led us to investigate amino acid frequency graphs to distinguish the characteristics for each data set. In the TiO_2[b] approach, basic amino acids R, K, and H were found to be overrepresented with varying degrees (Fig. 4A). In the Ti^{4+}-IMAC[b] data set, acidic amino acids D and E were more frequently enriched than the basic amino acids R, K, and H (Fig. 4B). One possible explanation is that HFP stretches the peptide backbone by breaking the intra-peptide ion interaction between negatively charged phosphate group and positively charged basic residues (31) such that the phosphate group can be more easily accessed by Ti^{4+}-IMAC. As a result, the chance of affinity interaction of acidic amino acids with Ti^{4+}-IMAC is also similarly increased. Apart from this, acidic residues such as aspartic acid and glutamic acid adjacent to tryptic cleavage sites can reduce the efficiency of trypsin digestion (38, 59, 60), resulting in miss-cleavages that increase the net charges of peptides. This also explains our observation that Ti^{4+}-IMAC[b] data set has the highest proportion of phosphopeptides with at least 1 mis-cleavage (62.1%) compared with Ti^{4+}-IMAC[a] (55.1%) and TiO_2[b] (52.4%). The basic amino acids R, K and H as well as acidic amino acids D and E are overrepresented in the pool after Ti^{4+}-IMAC[a] enrichment (Fig. 4C). Among the three methods, Ti^{4+}-IMAC[a] appears to contain to a large degree all populations enriched

by the use HFP and TiO_2 displaying thus the least bias. As mentioned earlier, the high content of TFA (6%) itself can reduce the level of intrapeptide bonding between positively charged basic residues and negative phosphate group (33) and aid coordination of the phosphate group to Ti^{4+}. The high level of TFA also aided the enrichment levels achieved by TiO_2 but not to the same extent. The superior results for positive phosphopeptides by Ti^{4+}-IMAC may be related to the use of a phosphate scaffold to immobilize the Ti^{4+} metal ion which is more resilient to the high levels of TFA and may also restrict the type of ligand that can coordinate and allow phosphate groups to be favored.

Identifying specific substrates of kinases is essential for constructing phosphorylation networks and understanding signal transduction in complex biological systems (62). Most interestingly, our data set (Fig. 5) shows that positive phosphopeptides recovered from the late SCX fractions contain relative higher occurrences of phosphopeptides originating from putative basophilic kinase substrates (63). Overall, the relative contribution of basophilic kinase substrate phosphopeptides was ~25% in the positive phosphopeptide data set compared with only 11% in the neutral phosphopeptide data set. In the positive phosphopeptides we detected the majority of putative PKA, AKT and AURORA substrates. These findings suggest that in SCX based large scale phosphoproteomics analysis, the late SCX fractions, which require high level of phosphopeptide enrichment, cannot be ignored especially not when one is interested for instance in cAMP/PKA (64), cGMP/PKG, AKT, or Aurora involved signaling. A bias toward analyzing only the early SCX fractions, which is quite common in current phosphoproteomic analysis, will negatively influence the outcome of such analysis.

For the systematic evaluation, all enriched positive phosphopeptides were analyzed by alternating CID and ETD and we also performed HCD, ETD, and CID for the triple dimethyl labeled sample. Using these datasets we were able to assess whether HCD, CID, or ETD is better-suited for phosphopeptide containing multiple basic residues. Our data revealed that, in particular, for the late SCX fractions ETD boosted the number of phosphopeptide identifications significantly (Fig. 3A, Fig. 6), in line with previous reports (38, 39, 45, 65, 66).

CONCLUSIONS

The data presented here indicate that a combination of SCX fractionation and Ti^{4+}-IMAC based enrichment, provides one of the most comprehensive phosphopeptide enrichment and analysis technologies up to date, enabling to further boost the number of phosphopeptide identifications in large scale phosphoproteomics analyses. The Ti^{4+}-IMAC method enhances in particular the recovery of positive phosphopeptides, containing multiple basic residues, but performed also well in neutral phoshopeptide enrichment. We exemplify our strategy by being able to generate over 9000 phosphorylation sites from a single experiment consisting of a triple dimethyl labeled ly-

sate. Therefore, we conclude that the Ti^{4+}-IMAC based enrichment technology may be an extremely valuable tool in the ever expanding field of phosphoproteomics.

REFERENCES

1. Hunter, T. (2000) Signaling–2000 and beyond. *Cell.* **100,** 113–127
2. Pawson, T., and Scott, J. D. (2005) Protein phosphorylation in signaling–50 years and counting. *Trends. Biochem. Sci.* **30,** 286–290
3. Dephoure, N., Zhou, C., Villén, J., Beausoleil, S. A., Bakalarski, C. E., Elledge, S. J., and Gygi, S. P. (2008) A quantitative atlas of mitotic phosphorylation. *Proc. Natl. Acad. Sci. U.S.A.* **105,** 10762–10767
4. Van Hoof, D., Muñoz, J., Braam, S. R., Pinkse, M. W., Linding, R., Heck, A. J., Mummery, C. L., and Krijgsveld, J. (2009) Phosphorylation dynamics during early differentiation of human embryonic stem cells. *Cell. Stem. Cell* **5,** 214–226
5. Olsen, J. V., Blagoev, B., Gnad, F., Macek, B., Kumar, C., Mortensen, P., and Mann, M. (2006) Global, in vivo, and site-specific phosphorylation dynamics in signaling networks. *Cell.* **127,** 635–648
6. White, F. M. (2008) Quantitative phosphoproteomic analysis of signaling network dynamics. *Curr. Opin. Biotechnol.* **19,** 404–409
7. Johnson, S. A., and Hunter, T. (2005) Kinomics: methods for deciphering the kinome. *Nat. Methods.* **2,** 17–25
8. Cohen, P. (2000) The regulation of protein function by multisite phosphorylation–a 25 year update. *Trends. Biochem. Sci.* **25,** 596–601
9. Ballif, B. A., Villén, J., Beausoleil, S. A., Schwartz, D., and Gygi, S. P. (2004) Phosphoproteomic analysis of the developing mouse brain. *Mol. Cell. Proteomics.* **3,** 1093–1101
10. Beausoleil, S. A., Jedrychowski, M., Schwartz, D., Elias, J. E., Villén, J., Li, J., Cohn, M. A., Cantley, L. C., and Gygi, S. P. (2004) Large-scale characterization of HeLa cell nuclear phosphoproteins. *Proc. Natl. Acad. Sci. U.S.A.* **101,** 12130–12135
11. Gauci, S., Helbig, A. O., Slijper, M., Krijgsveld, J., Heck, A. J., and Mohammed, S. (2009) Lys-N and trypsin cover complementary parts of the phosphoproteome in a refined SCX-based approach. *Anal. Chem.* **81,** 4493–4501
12. Alpert, A. J., Petritis, K., Kangas, L., Smith, R. D., Mechtler, K., Mitulović, G., Mohammed, S., and Heck, A. J. (2010) Peptide orientation affects selectivity in ion-exchange chromatography. *Anal. Chem.* **82,** 5253–5259
13. Gruhler, A., Olsen, J. V., Mohammed, S., Mortensen, P., Faergeman, N. J., Mann, M., and Jensen, O. N. (2005) Quantitative phosphoproteomics applied to the yeast pheromone signaling pathway. *Mol. Cell. Proteomics.* **4,** 310–327
14. Villén, J., and Gygi, S. P. (2008) The SCX/IMAC enrichment approach for global phosphorylation analysis by mass spectrometry. *Nat. Protoc.* **3,** 1630–1638
15. Pinkse, M. W., Mohammed, S., Gouw, J. W., van Breukelen, B., Vos, H. R., and Heck, A. J. (2008) Highly robust, automated, and sensitive online TiO2-based phosphoproteomics applied to study endogenous phosphorylation in Drosophila melanogaster. *J. Proteome Res.* **7,** 687–697
16. Benschop, J. J., Mohammed, S., O'Flaherty, M., Heck, A. J., Slijper, M., and Menke, F. L. (2007) Quantitative phosphoproteomics of early elicitor signaling in Arabidopsis. *Mol. Cell. Proteomics.* **6,** 1198–1214
17. Kweon, H. K., and Håkansson, K. (2006) Selective zirconium dioxide-based enrichment of phosphorylated peptides for mass spectrometric analysis. *Anal. Chem.* **78,** 1743–1749
18. Ficarro, S. B., Parikh, J. R., Blank, N. C., and Marto, J. A. (2008) Niobium(V) oxide (Nb2O5): application to phosphoproteomics. *Anal. Chem.* **80,** 4606–4613
19. Posewitz, M. C., and Tempst, P. (1999) Immobilized gallium(III) affinity chromatography of phosphopeptides. *Anal. Chem.* **71,** 2883–2892
20. Zhou, H., Xu, S., Ye, M., Feng, S., Pan, C., Jiang, X., Li, X., Han, G., Fu, Y., and Zou, H. (2006) Zirconium phosphonate-modified porous silicon for highly specific capture of phosphopeptides and MALDI-TOF MS analysis. *J. Proteome Res.* **5,** 2431–2437
21. Zhou, H., Ye, M., Dong, J., Han, G., Jiang, X., Wu, R., and Zou, H. (2008) Specific phosphopeptide enrichment with immobilized titanium ion affinity chromatography adsorbent for phosphoproteome analysis. *J. Proteome Res.* **7,** 3957–3967
22. McNulty, D. E., and Annan, R. S. (2008) Hydrophilic interaction chromatography reduces the complexity of the phosphoproteome and improves global phosphopeptide isolation and detection. *Mol. Cell. Proteomics.* **7,** 971–980
23. Albuquerque, C. P., Smolka, M. B., Payne, S. H., Bafna, V., Eng, J., and Zhou, H. (2008) A multidimensional chromatography technology for in-depth phosphoproteome analysis. *Mol. Cell. Proteomics.* **7,** 1389–1396
24. Alpert, A. J. (2008) Electrostatic repulsion hydrophilic interaction chromatography for isocratic separation of charged solutes and selective isolation of phosphopeptides. *Anal. Chem.* **80,** 62–76
25. Nühse, T. S., Stensballe, A., Jensen, O. N., and Peck, S. C. (2003) Large-scale analysis of in vivo phosphorylated membrane proteins by immobilized metal ion affinity chromatography and mass spectrometry. *Mol. Cell. Proteomics.* **2,** 1234–1243
26. Wiśniewski, J. R., Nagaraj, N., Zougman, A., Gnad, F., and Mann, M. (2010) Brain phosphoproteome obtained by a FASP-based method reveals plasma membrane protein topology. *J. Proteome Res.* **9,** 3280–3289
27. Dai, J., Wang, L. S., Wu, Y. B., Sheng, Q. H., Wu, J. R., Shieh, C. H., and Zeng, R. (2009) Fully automatic separation and identification of phosphopeptides by continuous pH-gradient anion exchange online coupled with reversed-phase liquid chromatography mass spectrometry. *J. Proteome Res.* **8,** 133–141
28. Thingholm, T. E., Jensen, O. N., Robinson, P. J., and Larsen, M. R. (2008) SIMAC (sequential elution from IMAC), a phosphoproteomics strategy for the rapid separation of monophosphorylated from multiply phosphorylated peptides. *Mol. Cell. Proteomics.* **7,** 661–671
29. Klemm, C., Otto, S., Wolf, C., Haseloff, R. F., Beyermann, M., and Krause, E. (2006) Evaluation of the titanium dioxide approach for MS analysis of phosphopeptides. *J. Mass. Spectrom.* **41,** 1623–1632
30. Wilson-Grady, J. T., Villén, J., and Gygi, S. P. (2008) Phosphoproteome analysis of fission yeast. *J. Proteome Res.* **7,** 1088–1097
31. Barnouin, K. N., Hart, S. R., Thompson, A. J., Okuyama, M., Waterfield, M., and Cramer, R. (2005) Enhanced phosphopeptide isolation by Fe(III)-IMAC using 1,1,1,3,3,3-hexafluoroisopropanol. *Proteomics.* **5,** 4376–4388
32. Iliuk, A. B., Martin, V. A., Alicie, B. M., Geahlen, R. L., and Tao, W. A. (2010) In-depth analyses of kinase-dependent tyrosine phosphoproteomes based on metal ion functionalized soluble nanopolymers. *Mol. Cell. Proteomics* 2162–2172
33. Mysling, S., Palmisano, G., Højrup, P., and Thaysen-Andersen, M. (2010) Utilizing ion-pairing hydrophilic interaction chromatography solid phase extraction for efficient glycopeptide enrichment in glycoproteomics. *Anal. Chem.* **82,** 5598–5609
34. Ficarro, S. B., McCleland, M. L., Stukenberg, P. T., Burke, D. J., Ross, M. M., Shabanowitz, J., Hunt, D. F., and White, F. M. (2002) Phosphoproteome analysis by mass spectrometry and its application to Saccharomyces cerevisiae. *Nat. Biotechnol.* **20,** 301–305
35. Boersema, P. J., Mohammed, S., and Heck, A. J. (2009) Phosphopeptide fragmentation and analysis by mass spectrometry. *J. Mass. Spectrom.* **44,** 861–878
36. Grimsrud, P. A., Swaney, D. L., Wenger, C. D., Beauchene, N. A., and Coon, J. J. (2010) Phosphoproteomics for the masses. *ACS. Chem. Biol.* **5,** 105–119
37. Schroeder, M. J., Shabanowitz, J., Schwartz, J. C., Hunt, D. F., and Coon,

J. J. (2004) A neutral loss activation method for improved phosphopeptide sequence analysis by quadrupole ion trap mass spectrometry. *Anal. Chem.* **76,** 3590–3598

38. Molina, H., Horn, D. M., Tang, N., Mathivanan, S., and Pandey, A. (2007) Global proteomic profiling of phosphopeptides using electron transfer dissociation tandem mass spectrometry. *Proc. Natl. Acad. Sci. U.S.A.* **104,** 2199–2204

39. Swaney, D. L., Wenger, C. D., Thomson, J. A., and Coon, J. J. (2009) Human embryonic stem cell phosphoproteome revealed by electron transfer dissociation tandem mass spectrometry. *Proc. Natl. Acad. Sci. U.S.A.* **106,** 995–1000

40. Chi, A., Huttenhower, C., Geer, L. Y., Coon, J. J., Syka, J. E., Bai, D. L., Shabanowitz, J., Burke, D. J., Troyanskaya, O. G., and Hunt, D. F. (2007) Analysis of phosphorylation sites on proteins from Saccharomyces cerevisiae by electron transfer dissociation (ETD) mass spectrometry. *Proc. Natl. Acad. Sci. U.S.A.* **104,** 2193–2198

41. Swaney, D. L., McAlister, G. C., and Coon, J. J. (2008) Decision tree-driven tandem mass spectrometry for shotgun proteomics. *Nat. Methods.* **5,** 959–964

42. Taouatas, N., Altelaar, A. F., Drugan, M. M., Helbig, A. O., Mohammed, S., and Heck, A. J. (2009) Strong cation exchange-based fractionation of Lys-N-generated peptides facilitates the targeted analysis of post-translational modifications. *Mol. Cell. Proteomics.* **8,** 190–200

43. Mischerikow, N., Altelaar, A. F., Navarro, J. D., Mohammed, S., and Heck, A. J. (2010) Comparative assessment of site assignments in CID and electron transfer dissociation spectra of phosphopeptides discloses limited relocation of phosphate groups. *Mol. Cell. Proteomics.* **9,** 2140–2148

44. Mohammed, S., and Heck, A., Jr. (2011) Strong cation exchange (SCX) based analytical methods for the targeted analysis of protein post-translational modifications. *Curr. Opin. Biotechnol.* **22,** 9–16

45. Domon, B., Bodenmiller, B., Carapito, C., Hao, Z., Huehmer, A., and Aebersold, R. (2009) Electron transfer dissociation in conjunction with collision activation to investigate the Drosophila melanogaster phosphoproteome. *J. Proteome Res.* **8,** 2633–2639

46. Pinkse, M. W., Uitto, P. M., Hilhorst, M. J., Ooms, B., and Heck, A. J. (2004) Selective isolation at the femtomole level of phosphopeptides from proteolytic digests using 2D-NanoLC-ESI-MS/MS and titanium oxide precolumns. *Anal. Chem.* **76,** 3935–3943

47. Boersema, P. J., Raijmakers, R., Lemeer, S., Mohammed, S., and Heck, A. J. (2009) Multiplex peptide stable isotope dimethyl labeling for quantitative proteomics. *Nat. Protoc.* **4,** 484–494

48. Yu, Z., Han, G., Sun, S., Jiang, X., Chen, R., Wang, F., Wu, R., Ye, M., and Zou, H. (2009) Preparation of monodisperse immobilized Ti(4+) affinity chromatography microspheres for specific enrichment of phosphopeptides. *Anal. Chim. Acta* **636,** 34–41

49. Thingholm, T. E., Jørgensen, T. J., Jensen, O. N., and Larsen, M. R. (2006) Highly selective enrichment of phosphorylated peptides using titanium dioxide. *Nat. Protoc.* **1,** 1929–1935

50. Raijmakers, R., Berkers, C. R., de Jong, A., Ovaa, H., Heck, A. J., and Mohammed, S. (2008) Automated online sequential isotope labeling for protein quantitation applied to proteasome tissue-specific diversity. *Mol. Cell. Proteomics* **7,** 1755–1762

51. Swaney, D. L., McAlister, G. C., Wirtala, M., Schwartz, J. C., Syka, J. E., and Coon, J. J. (2007) Supplemental activation method for high-efficiency electron-transfer dissociation of doubly protonated peptide precursors. *Anal. Chem.* **79,** 477–485

52. Savitski, M. M., Mathieson, T., Becher, I., and Bantscheff, M. H-score, a mass accuracy driven rescoring approach for improved peptide identification in modification rich samples. *J. Proteome Res.* **9,** 5511–5516

53. Frese, C. K., Altelaar, A. F., Hennrich, M. L., Nolting, D., Zeller, M., Griep-Raming, J., Heck, A. J., and Mohammed, S. (2011) Improved peptide identification by targeted fragmentation using CID, HCD and ETD on an LTQ-Orbitrap Velos. *J. Proteome Res.* **10,** 2377–2388

54. van den Toorn, H. W., Muñoz, J., Mohammed, S., Raijmakers, R., Heck, A. J., and van Breukelen, B. (2011) RockerBox: analysis and filtering of massive proteomics search results. *J. Proteome Res.* **10,** 1420–1424

55. Käll, L., Canterbury, J. D., Weston, J., Noble, W. S., and MacCoss, M. J. (2007) Semi-supervised learning for peptide identification from shotgun proteomics datasets. *Nat. Methods.* **4,** 923–925

56. Savitski, M. M., Lemeer, S., Boesche, M., Lang, M., Mathieson, T., Bantscheff, M., and Kuster, B. (2011) Confident phosphorylation site localization using the mascot delta score. *Mol. Cell. Proteomics* **10,** 1–12

57. Colaert, N., Helsens, K., Martens, L., Vandekerckhove, J., and Gevaert, K. (2009) Improved visualization of protein consensus sequences by ice-Logo. *Nat. Methods.* **6,** 786–787

58. Villén, J., Beausoleil, S. A., Gerber, S. A., and Gygi, S. P. (2007) Large-scale phosphorylation analysis of mouse liver. *Proc. Natl. Acad. Sci. U.S.A.* **104,** 1488–1493

59. Schlosser, A., Pipkorn, R., Bossemeyer, D., and Lehmann, W. D. (2001) Analysis of protein phosphorylation by a combination of elastase digestion and neutral loss tandem mass spectrometry. *Anal. Chem.* **73,** 170–176

60. Knight, Z. A., Schilling, B., Row, R. H., Kenski, D. M., Gibson, B. W., and Shokat, K. M. (2003) Phosphospecific proteolysis for mapping sites of protein phosphorylation. *Nat. Biotechnol.* **21,** 1047–1054

61. Cox, J., and Mann, M. (2008) MaxQuant enables high peptide identification rates, individualized p.p.b.-range mass accuracies and proteome-wide protein quantification. *Nat. Biotechnol.* **26,** 1367–1372

62. Linding, R., Jensen, L. J., Ostheimer, G. J., van Vugt, M. A., Jørgensen, C., Miron, I. M., Diella, F., Colwill, K., Taylor, L., Elder, K., Metalnikov, P., Nguyen, V., Pasculescu, A., Jin, J., Park, J. G., Samson, L. D., Woodgett, J. R., Russell, R. B., Bork, P., Yaffe, M. B., and Pawson, T. (2007) Systematic discovery of in vivo phosphorylation networks. *Cell.* **129,** 1415–1426

63. Hanks, S. K., and Hunter, T. (1995) Protein kinases 6. The eukaryotic protein kinase superfamily: kinase (catalytic) domain structure and classification. *FASEB J.* **9,** 576–596

64. Oberprieler, N. G., Lemeer, S., Kalland, M. E., Torgersen, K. M., Heck, A. J., and Taskén, K. (2010) High-resolution mapping of prostaglandin E2-dependent signaling networks identifies a constitutively active PKA signaling node in CD8+CD45RO+ T cells. *Blood.* **116,** 2253–2265

65. Frese, C. K., Altelaar, A. F., Hennrich, M. L., Nolting, D., Zeller, M., Griep-Raming, J., Heck, A. J., and Mohammed, S. (2011) Improved Peptide Identification by Targeted Fragmentation Using CID, HCD and ETD on an LTQ-Orbitrap Velos. *J. Proteome Res.* **10,** 2377–2388

66. Aguiar, M., Haas, W., Beausoleil, S. A., Rush, J., and Gygi, S. P. (2010) Gas-phase rearrangements do not affect site localization reliability in phosphoproteomics data sets. *J. Proteome Res.* **9,** 3103–3107